PHYSICAL REVIEW B VOLUME 52, NUMBER 7 15 AUGUST 1995-I

Electronic structure of intercalated graphite studied by soft-x-ray-emission spectroscopy

Guojiang Gu and S. E. Schnatterly
Jesse Beams Laboratory of Physics, University of Virginia, Charlottesville, Virginia 22901

(Received 13 February 1995)

Carbon K soft-x-ray-emission (SXE) spectra of highly ordered pyrolytic graphite (HOPG) and intercalated graphite with both donor (LiC_6) and acceptor ($FeCl_3$) doping are presented and compared. A numerical calculation using partially inverted initial states is carried out and models are constructed to fit these data using this method. It is shown that this approach is able to describe accurately the enhancement of the SXE spectrum near the Fermi energy for LiC_6. In the case of graphite intercalated with $FeCl_3$, the model also produces an enhanced Fermi edge while the data show no difference from the spectrum of HOPG. This aspect of the spectra of acceptor compounds is not at present understood.

INTRODUCTION

It is believed from many experimental[1,2] and theoretical[3,4] studies that, in alkali-metal–graphite intercalation compounds, the shape of the graphite density of states (DOS) remains largely unchanged upon intercalation and donor electrons from the alkali atoms are introduced into the previously empty carbon π^* antibonding conduction band, raising the Fermi level relative to that of graphite. Mansour and Schnatterly[5] carried out carbon K soft-x-ray-emission (SXE) measurements on highly ordered pyrolytic graphite (HOPG) and LiC_6 stage 1 intercalated graphite. The measurement and data analysis are described in detail in Ref. 5. Briefly, a series of the measurements of carbon k emission spectra of HOPG and LiC_6 were measured for different takeoff angles. These spectra are due to transitions of both σ and π valence electrons into the carbon 1s level. If θ is the takeoff angle measured from the c axis, then the π emission varies as $\sin2(\theta)$, and the σ emission varies as $[1+\cos2(\theta)]$. The σ and π bands were separated using the above relations. The π bands of HOPG and LiC_6 were obtained and Fig. 1 shows the π band of LiC_6 plotted on top of that of HOPG. The area under the HOPG π band is one electron and the area under the LiC_6 π band is 1.26 electrons. The transition density of states (TDOS) appears to show a charge transfer of 0.26 electrons per carbon atom greater than a complete charge transfer of 0.167 electrons, which is expected to be the case in LiC_6. Thus we observe an increase in the intensity seen in soft-x-ray emission near the Fermi energy of a factor of 1.56.

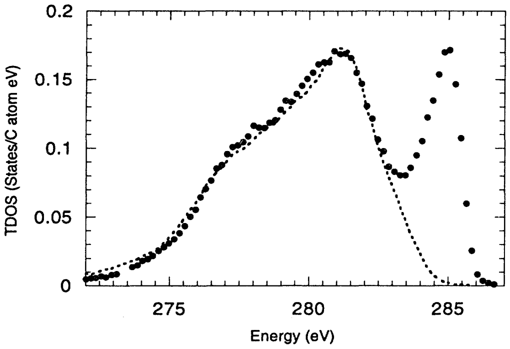

FIG. 1. π band of LiC_6 (dots) plotted on the top of that of HOPG (dashed line).

The enhancements near the Fermi edge in SXE spectra have been seen in many simple metals.[6,7] A many-body theory, known as MND theory, was developed by Mahan,[8] Nozières and De Dominicis,[9] and Combescot and Nozières[10] (MND) to explain these phenomena. In soft-x-ray emission, the sudden annihilation of the core hole causes a rearrangement of the electron wave functions near the Fermi energy so as to increase their overlap with the core hole.[5,11] Thus the transition density of states near the Fermi edge increases. A quantitative calculation of this enhancement can be carried out using appropriate correlation functions, the orthogonalized final state (OFS) approximation of Davis and Feldkamp,[12] or partially inverted initial states (PIIS) method of Livins and Schnatterly.[13] Dunlap, Ramaker, and Murday carried out a calculation of the TDOS appropriate for interpretation of Auger spectra[14] of LiC_6 using the OFS approximation. They expected the same enhancement factor of 4 in the SXE, which does not agree with our experiment. In fact, although the OFS approximation does include an edge enhancement, it gives a logarithmic singularity as demonstrated by Green.[15] In this paper, we used the partially inverted initial states method, which should produce the correct Mahan power-law singularity, to calculate the enhancement near the Fermi edge.

THEORY AND CALCULATION

For single-particle transitions, no electron-electron interaction, and a long-lived core state, the soft-x-ray-emission spectrum can be viewed as an angular momentum projection of the valence-electron density of states for a solid. One step beyond this simple approach is to take into account the different ionic potentials affecting the valence electrons when the core state is occupied or

0163-1829/95/52(7)/5298(4)/$06.00

empty. The work of Mahan, Nozières, De Dominicis, and Combescot provided a description of this problem with asymptotically exact solutions near the Fermi edge in metals. These methods involve the calculation of the appropriate correlation functions. Alternatively, one can consider the initial and final states constructed with Slater determinants. In considering this determinant, Davis and Feldkamp[12] noted that in a simple single-particle calculation it is a good approximation to use orthogonalized final state orbitals for the active electronic state (that state from which, in emission, the electronic transition occurs). For emission, the single-particle initial states ϕ are distorted due to existence of the vacant core level, while the final states ψ are the undistorted Bloch states. The OFS to use in the emission is given by

$$\begin{aligned} |\psi_i^{\rm OFS}\rangle &= |\psi_i\rangle - \sum_{j=M+1}^{N} \langle\phi_j|\psi_i\rangle|\phi_j\rangle \\ &= \sum_{j=1}^{M} \langle\phi_j|\psi_j\rangle|\phi_j\rangle \\ &= \sum_{j=1}^{M} S_{ji}^{-1}|\phi_j\rangle , \end{aligned} \tag{1}$$

where M denotes the number of occupied states, N the total number of states in the orthonormal set, and $S_{ji}^{-1}=\langle\phi_j|\psi_i\rangle$. As derived by Livins and Schnatterly,[13] the partially inverted initial state is given by

$$|\psi_i^{\rm PIIS}\rangle = \sum_{j}^{M} s_{ji}^{-1}|\phi_j\rangle . \tag{2}$$

The distinction between the OFS and PIIS lies entirely in whether one uses the inverse of the full matrix S, or the inverse of the smaller occupied submatrix s.

A simple model system, in which a numerical investigation of the ideas discussed in the preceding section is possible, can be found in the spherical square well. Different angular components are completely decoupled, thus simple s wave solutions, confined to a sphere with radius R, suffice in the construction of two orthonormal complete sets of wave functions. One set, the undistorted set, corresponds to the completely free particle with wave function

$$\psi_n(r) = A\frac{\sin(kr)}{kr}, \quad k = n\pi/R . \tag{3}$$

The distorted set, corresponding to a well depth V_0 and radius a in the center of the sphere, has a wave function

$$\begin{aligned} \phi_m(r) &= A'\left[b\frac{\sin(k'r)}{k'r} - c\frac{\cos(k'r)}{k'r} \right] \\ &\qquad \text{for } r > a \ (k' = m\pi/R - \delta/R) , \\ \phi_m(r) &= A'\frac{\sin(k_0 r)}{k_0 r} \\ &\qquad \text{for } r < a \ \left[k_0 = \left[k'^2 + \frac{2mV_0}{h^2} \right]^{1/2} \right] , \end{aligned} \tag{4}$$

where A and A' are normalization coefficients, n and m are integers, and $\delta = -\arctan(c/b)$ is the phase shift. The coefficients b and c are determined by V_0, a, and R. The occupied inverted matrix $s_{mn}^{-1} = \langle\phi_m|\psi_n\rangle$ can be constructed using Eqs. (3) and (4) and partially inverted states can be constructed using Eq. (2).

The observed soft-x-ray-emission intensity may be written as a transition rate $T(\gamma)$:

$$T(\gamma) \sim \sum_f \gamma \left| \left\langle \Psi_f \left| \sum_j \mathbf{AP}_j \right| \Psi_i \right\rangle \right|^2 \delta(E_i - E_f - \gamma) , \tag{5}$$

where Ψ_i with E_i and Ψ_f with E_f are the initial and final many-body electronic states and energies, respectively, while γ is the photon frequency. This expression can be further simplified as

$$T(E) \sim \gamma^3 N(E) |\langle c|\mathbf{r}|\Psi(\mathbf{k})\rangle|^2 , \tag{6}$$

where $N(E)$ is the total density of states, $|c\rangle$ the core state, and $|\Psi(\mathbf{k})\rangle$ a Bloch state with wave vector $\mathbf{k}$. For this matrix element we follow Von Barth and Grossman[16] and also Mahan,[17] and use

$$\langle c|\mathbf{r}|\Psi\rangle = \int \Psi(\mathbf{r})\exp(-r/r_c)d\mathbf{r} , \tag{7}$$

where r_c represents some suitable core radius. $\psi^{\rm PIIS}(\mathbf{r})$ is used for the Bloch state $|\Psi(\mathbf{r})\rangle$ to evaluate the many-body enhancement effects.

The soft-x-ray spectra for simple metals can be obtained with correct enhancements near the Fermi edge by evaluating Eq. (6). For example, we use a well depth $V_0 = 12$ eV, width $a = 0.8$ Å, and a Fermi energy of 3.13 eV, corresponding to sodium to describe sodium SXE data. Using 80 occupied states exhausts the sum rule by better than 99%. The calculated spectrum fits the soft-x-ray-emission data for the sodium well.[18]

However, in order to apply this calculation to alkali-metal–graphite intercalation compounds to explain the enhancement near the Fermi edge, we have to extend this

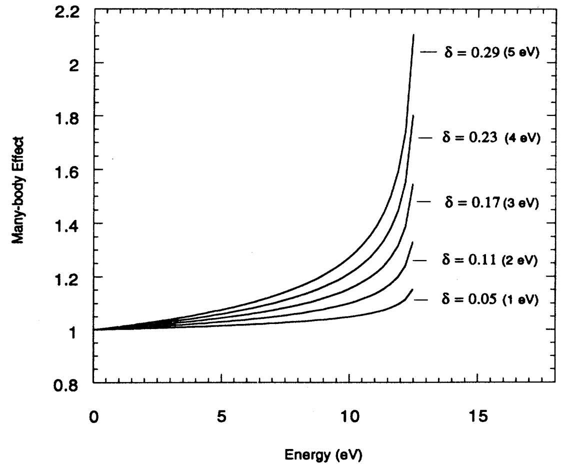

FIG. 2. Many-body enhancement with different core potential strengths; δ is the phase shift at the Fermi energy.

calculation because of the rapid variation of the density of states near E_F for these materials. A simple step is to take the ratio of a spectrum with some core potential strength and a spectrum without a potential well in the center. Figure 2 shows these ratios with different potential strengths V_0 from 1.0 to 5.0 eV. We choose a Fermi energy of 12.5 eV, corresponding to the E_F of HOPG, and core radius of 0.087 Å, corresponding to the carbon 1*s* core level.[19] We can see that the many-body effect is very weak far away from the Fermi edge, while its intensity increases approaching the Fermi level. The bigger the potential strength, the stronger the many-body effect.

RESULTS AND DISCUSSION

We construct the initial DOS for HOPG as follows. We use three straight line segments resembling the soft-x-ray-emission spectrum of HOPG from 272 to 281.25 eV. The many-body effect is very weak far away from the Fermi edge so this part of the spectrum is unaffected by it. A curve whose curvature is the same as that of the curve near the Fermi edge in the DOS of HOPG calculated by Weinberger *et al.*[20] is used for the initial DOS from 281.25 to 284 eV. Then we calculate the many-body enhancement effect for HOPG as shown in Fig. 2 with a potential well depth $V_0 = 2.3$ eV, which will be explained later. We multiply this rigid band model (the initial DOS) by the many-body enhancement effect and convolute the product with a Gaussian broadening function with a standard deviation of 0.31 eV. The result fits the soft-x-ray-emission spectrum for HOPG quite well. We notice that the enhancement effect does not dominate the spectrum near the Fermi edge since the density of states of the valence band of graphite approaches zero at the Fermi energy.[20]

The initial DOS of LiC_6 is constructed as shown by dashed line in Fig. 3(a). We locate a point on the slope of the initial DOS of HOPG near the Fermi energy according to the minimum position shown in the SXE data of LiC_6. From this point, we build the π^* band in such a way that the π band and π^* band are symmetric about the minimum point and that the π^* band is extended to the point where the total area under the curve is 1.17, which is consistent with a total charge transfer from Li to carbon atoms. As we did for HOPG, we multiply this model by the many-body enhancement effect and adjust the potential strength so that the enhanced model as an area of 1.26. Then the model is convoluted with a Gaussian function with the same standard deviation as for the HOPG model. The solid line in Fig. 3(a) shows the enhanced model with a potential well depth of $V_0 = 2.3$ eV. Figure 3(b) shows the broadened enhanced model and we can see that it also fits the LiC_6 data quite well. However, we notice that the largest discrepancy between these experimental results and calculations of the density of states in these compounds[3] occurs in the region of the minimum near 282.5 eV. The calculated value of the minimum DOS is 0.015 states/(carbon atom eV) while our observed value is about 0.08 states/(carbon atom eV). Some of this difference is due to the various sources of broadening not included in the calculation. However,

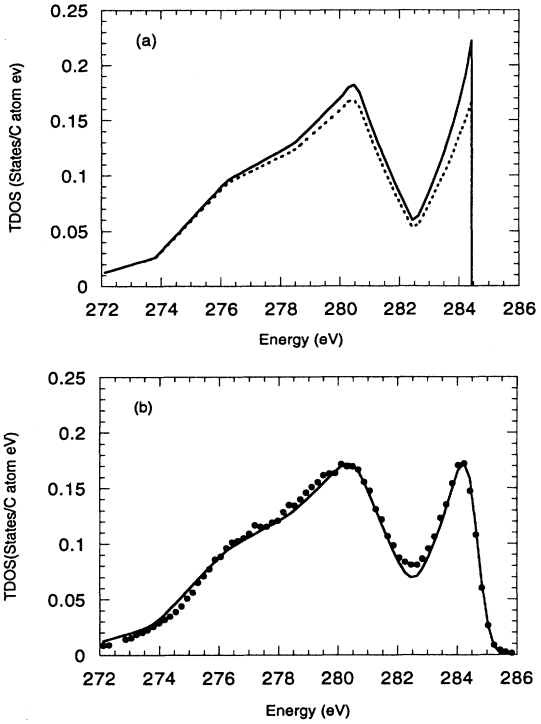

FIG. 3. (a) The dashed line is the starting model for LiC_6. The solid line is the enhanced model. (b) The dots are SXE data of LiC_6, and the solid line is the fit.

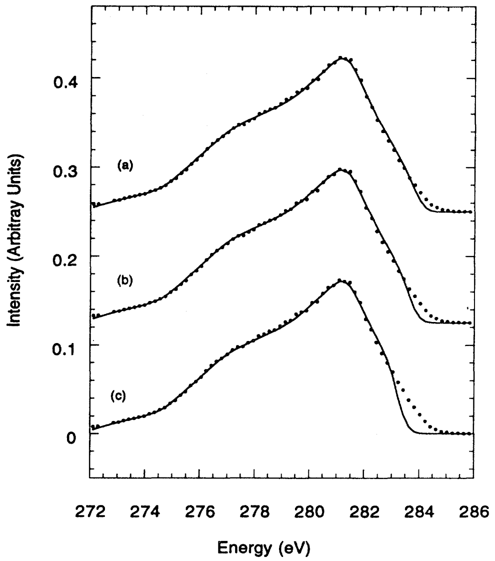

FIG. 4. The dots are SXE data of HOPG, and the solid lines in (a), (b), and (c) are the predicted SXE spectra with the Fermi energy shifts of 0.7, 0.9, and 1.3 eV, corresponding to charge transfer per carbon of 0.009, 0.016, and 0.025, respectively.

broadening is not sufficient to account for all of the difference.

Generally, appropriately enhanced models agree well with the SXE spectra for donor compounds. We should also be able to understand the spectra of acceptor compounds in the same way. For typical graphite acceptor compounds, the estimated Fermi energy reduction due to charge transfer away from the carbon atoms varies from 0.7 to 1.3 eV.[21] In order to apply our model to graphite acceptor compounds, we use the same initial DOS as we use for HOPG except that we cut off the DOS below the original Fermi energy. Then we include the many-body enhancement and Gaussian broadening with the same parameters as we used for both HOPG and LiC_6. Figure 4 shows the models with the Fermi energy shifts of 0.7, 0.9, and 1.3 eV compared with soft-x-ray-emission data of HOPG. For a Fermi energy shift of 0.7 eV, corresponding to 0.9% charge transfer per carbon atom, we notice that the curvature of the model near the Fermi energy changes from concave to convex and a shoulderlike structure starts to appear. This enhanced Fermi edge is more prominent and visible for Fermi energy shifts of 0.9 and 1.3 eV.

The lowering of the Fermi energy about 0.9 eV in stage-1 $FeCl_3$-intercalated graphite was directly measured in the electron-energy-loss spectrum by Mele and Ritsko.[22] So we expect the $FeCl_3$-intercalated graphite SXE data to look like curve (b) in Fig. 4. However, the soft-x-ray-emission data of $FeCl_3$-intercalated graphite show no difference from HOPG data.[23] Other soft-x-ray spectra of $FeCl_3$-intercalated graphite[24] and a range of other acceptor compounds such as $AlCl_3$ and SbF_5 intercalated compounds also showed no visible change from HOPG. We have no explanation for what appears to be a general result: Donor graphite intercalated compounds show the expected enhancement in soft-x-ray-emission spectra near the Fermi energy; acceptor compounds not only do not show enhancement, they do not even exhibit the expected charge-transfer effects. It is as though the charge that transferred away from the carbon atoms returns as the screening charge when a core hole is created on a carbon atom. Such a charge transfer would not, however, be part of the final state and so should not contribute to the measured spectrum. Compounds with fragile valence appear to have more complex shapes near threshold than are included in the present MND model. More careful experimental and theoretical studies on graphite acceptor compounds need to be done.

ACKNOWLEDGMENT

This work was supported in part by the National Science Foundation, Division of Materials Research Program under Grant No. DMR-9120055.

---

[1] I. T. McGovern, W. Eberhardt, E. W. Plummer, and J. E. Fischer, Physica B **99**, 415 (1990).

[2] P. Pfluger, P. Oelhafen, H. U. Kunzi, R. Jeker, E. Hauser, K. P. Ackermann, M. Muller, and H. J. Guntherodt, Physica B **99**, 395 (1980).

[3] N. A. W. Holzwarth, S. Rabii, and L. A. Girifalco, Phys. Rev. B **18**, 5190 (1978).

[4] N. A. W. Holzwarth, L. A. Girifalco, and S. Rabii, Phys. Rev. B **18**, 5206 (1978).

[5] A. Mansour and S. Schnatterly, Phys. Scr. **35**, 595 (1987).

[6] H. Needdermeyer, Phys. Rev. B **13**, 2411 (1976).

[7] P. A. Bruhwiler and S. E. Schnatterly, Phys. Rev. B **41**, 8013 (1990).

[8] G. D. Mahan, Phys. Rev. **163**, 612 (1967).

[9] P. Nozières and C. T. De Dominicis, Phys. Rev. **178**, 1097 (1968).

[10] M. Combescot and P. Nozières, J. Phys. (Paris) **32**, 913 (1971).

[11] A. Mansour, S. Schnatterly, and J. J. Risko, Phys. Rev. Lett. **58**, 614 (1987).

[12] L. C. Davis and L. A. Feldkamp, Phys. Rev. B **23**, 4269 (1981).

[13] P. Livins and S. E. Schnatterly, Phys. Rev. B **37**, 6731 (1987); **37**, 6742 (1987).

[14] B. I. Dunlap, D. E. Ramakre, and J. S. Murday, Phys. Rev. B **25**, 6439 (1982).

[15] T. A. Green, Phys. Rev. B **32**, 3442 (1985).

[16] U. Von Barth and G. Grossman, Phys. Rev. B **25**, 5150 (1982).

[17] G. D. Mahan, Phys. Rev. B **21**, 1421 (1980).

[18] P. Livins, Ph.D. thesis, University of Virginia, 1988.

[19] Frank Herman and Sherwood Skillman, *Atomic Structure Calculations* (Prentice-Hall, Englewood Cliffs, NJ, 1963).

[20] B. R. Weinberger, J. Kaufer, A. J. Heeger, J. E. Fischer, M. Moran, and N. A. W. Holzwarth, Phys. Rev. Lett. **41**, 1417 (1978).

[21] J. Blinowski, Nguyen Hy Hau, C. Rigaux, Jo P. Vieren, R. Le Toullec, G. Furdin, A. Herold, and J. Merlin, J. Phys. (Paris) **41**, 57 (1980).

[22] Eugene J. Mele and John J. Risko, Phys. Rev. Lett. **43**, 68 (1979).

[23] Fred J. Zutavern, Ph.D. thesis, Princeton University, 1982.

[24] R. Oisberg and G. Wiech, Synth. Met. **23**, 183 (1988).